Photocatalytic degradation evaluation using ternary structures of titanium dioxide, silver and carbon quantum dots

Lucca S. I. Omori, Luiz G. Sakaguti, Leonardo Z. Fogaça, Wilker Caetano, Monique de Souza, Mauro L. Baesso, Vagner R. Batistela, Mara H. N. O. Scaliante*.

L. S. I. Omori, State University of Maringá (UEM), Maringá, PR, 87020-900 BRAZIL (e-mail: luccaomori@gmail.com, ORCID: 0009-0006-8730-9984). L. G. Sakaguti, State University of Maringá, Maringá, PR 87020-900 BRAZIL (e-mail: lgsakaguti@gmail.com, ORCID: 0000-0002-0005-5461). L. Z. Fogaça, State University of Maringá, Maringá, PR 87020-900 BRAZIL (e-mail: lzfogaca@gmail.com, ORCID: 0000-0002-9250-3355). W. Caetano, State University of Maringá, Maringá, PR 87020-900 BRAZIL (e-mail: wcaetano@uem.br, ORCID: 0000-0002-9402-8324). M. de Souza, State University of Maringá, Maringá, PR 87020-900 BRAZIL (email: monikdsouza@hotmail.com, ORCID: 0000-0002-1340-1001). M. L. Baesso State University of Maringá, Maringá, PR 87020-900 BRAZIL (email: mlbaesso@dfi.uem.br, ORCID: 0000-0001-6017-2582). V. R. Batistela, State University of Maringá, Maringá, PR 87020-900 BRAZIL. (e-mail: vrbatistela@uem.br, ORCID: 0000-0001-8151-8765). M. H. N. O. Scaliante, State University of Maringá, Maringá, PR 87020-900 BRAZIL. (e-mail: mhnoscaliante2@uem.br, ORCID: 0000-0001-9090-9274)

DOI: https://doi.org/10.34024/jsse.2024.v2.19395

***Abstract*— The catalytic photodegradation of organic pollutants offers an eco-friendly alternative for improving water quality by reducing the use of strong oxidants. This method is particularly promising in dealing with organic pollutants that cannot be completely removed through traditional methodologies. However, limitations of the main photocatalysts used, such as high bandgap value and electronic recombination, present challenges for upscaling applications. In this study, photocatalytic heterostructures were synthesized using TiO_2 P25, carbon quantum dots (CQDs, average size: 4.9 nm, measured by DLS), and silver (Ag) to enhance photocatalytic performance and overcome these limitations. XRD analysis confirmed the successful incorporation of silver into the material, as evidenced by the presence of silver oxide peaks in the diffractogram. Photoacoustic spectroscopy demonstrated that the addition of CQDs reduced the bandgap energy of pure TiO_2 from 3.00 eV to 2.97 eV. The photolysis study revealed low kinetic constants for the reaction, with a value of 2.17×10^{-3} min^{-1}. For pure TiO_2, the kinetic constant was 3.82×10^{-2} min^{-1}. In contrast, the synthesized catalysts showed significantly higher kinetic constants of 3.52×10^{-1} min^{-1} for the catalyst containing only CQD and 1.75×10^{-1} min^{-1} for the heterostructure containing both CQD and Ag. These values represent notable improvements compared to pure TiO_2, with increases of 827% and 400%, respectively. The enhanced photocatalytic activity is attributed to the superior electronic transfer properties, diminished availability of recombination sites, efficient generation of oxidative radicals, and the improved interaction between the catalyst and the organic pollutant.**

***Keywords*—carbon quantum dots, catalytic photodegradation, heterogeneous photocatalysis.**

I. Introduction

The rapid pace of global industrialization has increased concern about water quality particularly due to the worrying issue of contamination in water bodies. Among these pollutants, organic dyes are particularly problematic as they are widely used across many different industries such as plastics, textiles and cosmetics [1]. Conventional treatment methods often fail to remove them efficiently resulting in their constant accumulation in the environment. This can lead to potential health problems, in particular living organisms and even whole ecosystems, especially as it hinders plant life. [2]

Currently, photocatalysis is garnering significant interest among researchers as a promising method for the removal of pollutants in water bodies. This is because, through advanced oxidation processes (AOPs), photocatalysis can mineralize complex organic compounds, transforming them into CO_2 and H_2O, thereby preventing the formation of residues or the generation of by-products that may be even more harmful than the precursor molecule [3].

Among the potential catalysts, TiO_2 stands out for its low cost, high stability, non-toxicity, high photocatalytic activity, and wide bandgap, allowing for a broad range of photocatalytic reactions [4]. However, challenges such as the high bandgap value and electronic recombination limit the large-scale use of photocatalysis in effluent treatment [5]. Numerous scientific studies are aiming to overcome these limitations. A promising solution is the addition of cocatalysts that, in a heterostructure with the semiconductor, exhibit synergistic behavior, reducing the bandgap and electronic recombination.

Carbon quantum dots (CQDs), with their zero-dimensional (0D) structure, sizes up to 10 nm, and unique characteristics such as high electronic mobility, up-conversion effect, and zero bandgap, enable much more efficient charge transport in

Paper submitted for review on 08/29/2024. This work was supported in part by Brazil's National Council for Scientific and Technological Development (CNPq).

heterostructures compared to the pure semiconductor [6].

The use of CQD as a cocatalyst offers several advantages over other potential cocatalysts. First, the high availability of carbon-based materials that can be used as precursors for the synthesis, such as lignin, the second most abundant biopolymer, typically burned in recovery boilers at paper and pulp mills, makes this approach attractive [7]. Additionally, relatively simple bottom-up methods, such as hydrothermal processes, can be used to produce CQD [8].

Noble metals also have widespread applications in photocatalysis, as studies demonstrate their ability to reduce the bandgap in heterostructures and prevent electronic recombination through electron trapping caused by the Schottky barrier [9]. Among them, silver stands out due to its low cost while maintaining a high performance, as evidenced by its effectiveness in the reduction reactions of p-nitrophenol [10].

Furthermore, the usage of metal-doped photocatalysts has also been studied in water splitting applications. Photoluminescence spectroscopy of these heterostructures reveals that the introduction of the metals reduces the intensity of luminescence spectra, indicating a significant decrease in electronic recombination rates and thus a greater reaction rate [11]. Both reports validate the versatility of heterostructures in photocatalytic reactions and highlight their significant potential in advancing this field.

Therefore, the present study aims to evaluate the photocatalytic performance and characterization of heterostructures composed of TiO_2, Ag, and CQD derived from commercial biomass, examining the influence of each cocatalyst on the semiconductor's performance.

II. Experimental

Synthesis of CQD

The synthesis of CQD was adapted from [12]. First, 3 g of alkaline lignin (Sigma-Aldrich) was dispersed in 100 mL of a solution containing 17% HNO_3. This solution was stirred for 6 hours at 80°C in a glycerin bath. After cooling to room temperature, the acidified lignin was obtained by vacuum filtration using filter paper with a medium pore size of 8 µm. The solid retained on the filter was then dried in an oven at 60°C overnight. The dried, acidified lignin was subsequently added to a 0.2 $mol \cdot L^{-1}$ NaOH solution and subjected to ultrasonication for 3 hours. After this, the solution was transferred to a Teflon container, which was placed in an autoclave and heated in an oven for 8 hours at 160°C. Finally, the post-hydrothermal process solution was vacuum-filtered through a 0.22 µm filter to remove impurities. The filtrate was collected and designated as CQD.

Synthesis of Photocatalysts

In this stage, three systems were developed using 2 g of TiO_2 P25 (Evonik). Two systems were added to 50 mL of deionized water, and the remaining one to a 0.01 M $AgNO_3$ solution. One system with deionized water and the system with $AgNO_3$ were both doped with 1.5% w/w CQD. The $AgNO_3$ system was exposed to UVC light for 1 hour to decompose the $AgNO_3$ and reduce the Ag^+. Afterward, the systems containing deionized water were subjected to a hydrothermal process at 160°C for 4 hours. All catalysts were dried in an oven at 60°C for 12 hours and labeled TiO_2HT, TiO_2/CQD, and TiO_2/CQD/Ag.

Photocatalytic Degradation

In the experiments were utilized a solution with 0.2 $g \cdot L^{-1}$ of catalyst and 3 mL of methylene blue (MB) 8.5×10^{-6} M in a quartz cuvette. The solution was kept in the dark for 30 minutes with agitation to stabilize the adsorption, followed by irradiation with UVA LED (5 W and λ = 365 nm) for 60 minutes. Absorbance was measured at 665 nm at predetermined intervals up to 60 minutes, using a Shimadzu UV-1800 spectrophotometer.

Characterization

The crystalline structure of materials was investigated using X-ray Diffraction (XRD) patterns XRD-6000, Shimadzu (Ni-filtered CuK, λ = 0.15418 nm, 40 kV, 30 mA, 0.02° resolution and 2° min−1 scanning speed) to identify the impregnation of CQD nanoparticles in crystallographic planes of TiO_2. The photoacoustic spectra were obtained in an experimental homemade spectrometer [13] exciting the catalyst with 800 W lamp with a 13 Hz modulation frequency, to determinate the reducing in band-gap values among the presence of carbon material and the TiO_2. TEM images were performed using a transmission electron microscope JEOL JEM-1400. The images were taken by applying an electron beam with 10–15 kV.

For the results obtained through the photoacoustic spectroscopy technique, the bandgap energy was calculated using the Tauc relation:

$$(\alpha h\nu) \propto \left(h\nu - E_g\right)^{\frac{1}{2}} \quad (1)$$

The value of 1/2 for the exponent in (1), refers to direct allowed transitions.

III. Results and Discussion

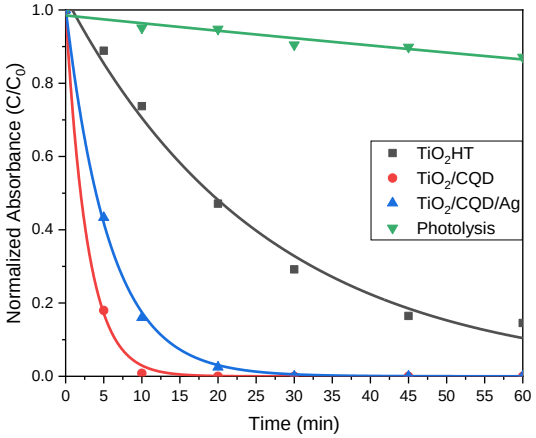

Fig. 1. Average curves fitted to the photocatalytic degradation reaction of methylene blue (MB) 8.5 × 10⁻⁶ M, using photolysis and 0.2 g·L⁻¹ of each catalyst.

The kinetic curves of catalytic photodegradation were averaged across replicates and are represented in Fig. 1. The graph reveals a significant difference in the concentration decay rate between the synthesized catalysts, the commercial catalyst (TiO_2HT), and the photolysis process. Notably, among the heterostructures prepared, the TiO_2/CQD/Ag system displayed a slower kinetic profile, indicating that the silver concentration used was harmful to the reaction under study.

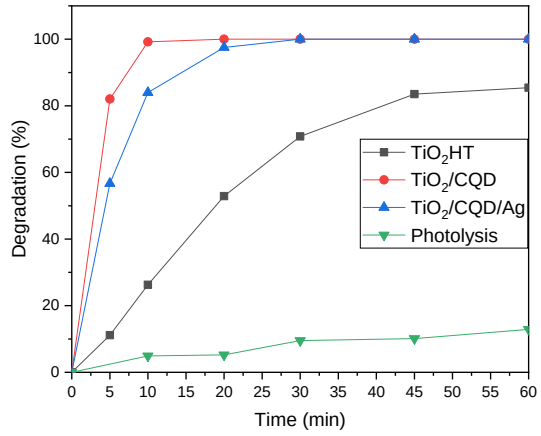

Fig. 2. Average degradation for photocatalytic reaction of methylene blue (MB) 8.5 × 10⁻⁶ M, using photolysis and 0.2 g·L⁻¹ of each catalyst.

Based on Fig. 2, it is observed that the TiO_2/CQD and TiO_2/CQD/Ag catalysts achieved 100% degradation within 20 and 30 minutes of reaction, respectively. In contrast, the TiO_2HT catalyst was unable to achieve complete degradation within the studied reaction time, reaching a degradation of 85%. Finally, photolysis proved to be inefficient, achieving only 13% degradation.

Reference [14] employs a mini-photoreactor similar to the one used in the present study. In this setup, a direct UVA reaction source is utilized, which, despite its low power (5 W) and short reaction times, still achieves efficient results with the catalysts employed. Additionally, the low catalyst concentration used (0.2 g·L⁻¹) enables direct spectrophotometric readings from the cuvette without the need for filtration, as previously studied by the same authors. Moreover, the concentration used also reflects the optimal catalyst proportion for the reaction under study.

During the initial 30 minutes without UV light exposure, adsorption was negligible across all catalyst-containing systems, as the system's turbidity hindered accurate concentration measurements. Consequently, it can be inferred that the studied systems possess a low number of active sites conducive to adsorption.

TABLE I
Parameters Related to Catalytic Photodegradation

Catalyst	k (min^{-1})	R^2	Gain [a] (%)	Degradation (%)
Photolysis	0.00217 ± 0,00031	0.906	-94	13
TiO_2HT	0.0382 ± 0.0024	0.989	-	85
TiO_2/CQD	0.352 ± 0.011	>0.999	821	100
TiO_2/CQD/Ag	0.175 ± 0.004	>0.999	358	100

[a] The gains are in relation to the commercial form of the catalyst (TiO_2HT)

The data gathered from the kinetics of the photodegradation reactions of methylene blue (Fig. 1) are presented in Table I. The pseudo-first-order fit proved to be satisfactory, as all systems containing the catalysts showed an R^2 greater than 0.98, ensuring the stability of the system throughout the reaction time.

After a thorough analysis of the obtained values, it is noted that TiO_2/CQD showed a significant improvement in the reaction rate. As shown by reference [15], this enhancement can be attributed to the high electronic mobility of the carbonaceous material, which facilitates effective charge separation within the heterostructure and therefore reducing the electronic recombination of TiO_2.

Although overall adsorption was negligible, the carbon structure of the CQDs facilitated interactions with the organic molecules of the dye enhancing their affinity [16]. Moreover, the high surface area, as a result from the reduced particle size of the CQDs, contributes to a higher contact area between the pollutant and the heterostructure. The increased adsorption positively influenced the reaction rate. These findings reaffirm that incorporating CQDs into photocatalysts can be highly advantageous, highlighting their synergistic effects of the heterostructure [17].

In contrast, silver exhibited an effect that reduced the reaction kinetics. This behavior may be attributed to the high concentration of silver used, which could have led to the formation of clusters that act as centers for electronic

recombination [16]. Additionally, the excess silver might create a physical barrier, hindering the interactions between the photocatalyst containing CQD and the dye, thus necessitating further studies to determine the ideal proportions of silver in the heterostructure.

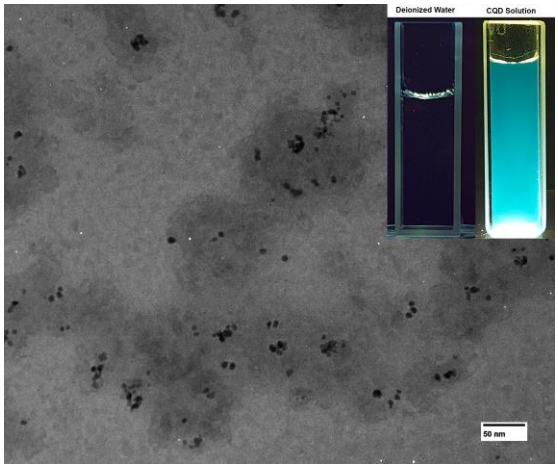

Fig. 3. TEM image and luminescence (irradiated by UVA LED 365 nm) of the CQD solution.

TABLE II
PARAMETERS RELATED TO DIAMETER OF THE CQD

Characterization	Observation	Diameter (nm)
DLS	D (10%)	4.1
	D (50%)	4.6
	D (90%)	5.3
	Average	4.9
TEM	-	8.427 ± 3.811

Transmission Electron Microscopy (TEM) of the CQD (Fig. 3) revealed the presence of both agglomerated and dispersed particles in its structure. For particle size evaluation, the ImageJ software (2023) was used, measuring the largest, smallest, and average particle sizes based on the image scale. A total of 161 particles were observed, with sizes ranging from 2.486 nm to 31.076 nm and an average particle size of 8.427 ± 3.811 nm. These results were compared with a DLS analysis conducted 12 months after the synthesis of the CQD, which presented an average particle size of 4.9 nm, demonstrating high material stability. All results related to the diameter of the CQD are presented in Table II. A small difference in particle size results can be observed, likely due to the method of grid preparation, where particles tended to agglomerate. Nevertheless, both methods indicate sizes of less than 10 nm, consistent with the requirement for CQDs to exhibit quantum effects as noted by [17].

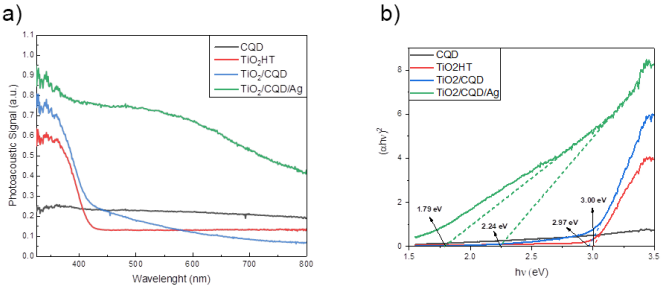

Fig. 4. a) Photoacoustic spectroscopy results of the CQD and catalysts (TiO_2HT, TiO_2/CQD and TiO_2/CQD/Ag). b) Tauc plot of the CQD and catalysts (TiO_2HT, TiO_2/CQD and TiO_2/CQD/Ag).

When evaluating the results of the photoacoustic spectroscopy analysis, represented in Fig. 4a, it can be observed that the CQD demonstrated a relatively low intensity compared to other materials. However, the material showed light absorption throughout the entire spectrum, exhibiting behavior different from that of a semiconductor due to the presence of quantum effects.

Through Fig. 4b, it can be observed that the TiO_2/CQD catalyst showed a reduction in bandgap energy when CQD was added (2.97 eV) compared to TiO_2HT (3.00 eV). Furthermore, the TiO_2/CQD/Ag photocatalyst demonstrated an even greater shift in radiation absorption capacity. However, the broad absorption range resulted in the absence of sharp edges in the Tauc plot graph. Thus, it can be estimated that the actual bandgap of the silver-containing catalyst is within the range of the sections that best fit straight lines, therefore, in this case, between 1.79–2.24 eV [18][19][20].

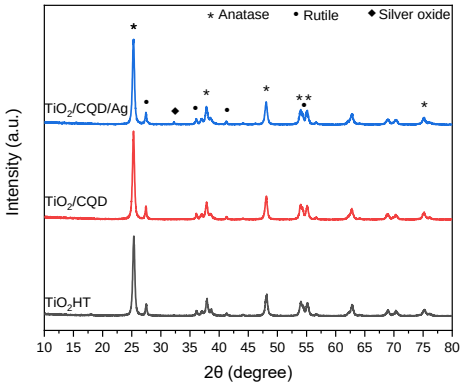

Fig. 5. XRD results.

The peak analysis presented by XRD (Fig. 5) was compared with the Crystallography Open Database (COD) entries, data nos. 7206075 and 9015662, representing the anatase and rutile phases, respectively. Using the classical relationship proposed by [21], the proportion of crystalline phases in the material was verified. In the original TiO_2 P25, an 80:20 ratio of anatase to rutile phases is typically observed. It was found that all synthesized catalysts exhibited an 89:11 ratio between the anatase and rutile phases, indicating a change in phase proportion, though not significant enough to notably impact the photocatalytic reactions when compared to the commercial P25

form. Additionally, at a 2θ angle of 32.25°, a small peak was observed for the catalyst containing silver [22]. This peak indicates the presence of silver oxide in the material rather than metallic silver in the heterostructure. This suggests the need for further procedures to convert silver oxide into metallic silver. However, redox reactions occurring in the reaction medium itself may lead to the *in-situ* reduction of silver, potentially eliminating the need for additional synthesis steps.

IV. Conclusion

The CQD in the structure demonstrated a significant enhancement in the photodegradation reactions, with the TiO_2/CQD heterostructure exhibiting the best performance with an 827% improvement compared to the photocatalyst containing only the TiO_2. In contrast, incorporating silver into the system negatively affected performance, reducing the kinetic response, although it still remained considerably more efficient than the initial catalyst with the commercial TiO_2 by a factor of 400%.

Furthermore, structural studies allowed for a comparison of particle sizes using different methodologies. Despite a slight discrepancy, the particle sizes remained within the range necessary to observe quantum effects. Moreover, the XRD analysis further confirmed that the synthesis process did not have a meaningful change in the proportion of crystalline phases when compared to TiO_2 P25.

Overall, the enhancements that both heterostructures provided to the pure catalyst were evident. These results strongly indicate that incorporating cocatalysts, such as carbonaceous materials and noble metals, into semiconductors is an extremely promising approach to overcome their inherent limitations. The findings from this study, therefore, provide valuable insights into the development of technologies aimed at achieving high-efficiency photocatalysts.

Acknowledgment

The authors would like to thank Brazil's National Council for Scientific and Technological Development (CNPq), Higher Education Personnel Improvement Coordination (CAPES), and Araucária State of Parana Research Foundation (Fundação Araucária) for financial support and the utilization of the Complex of Research Support Center of the State University of Maringá (COMCAP-UEM), the Laboratory of Adsorption and Ion Exchange of the State University of Maringá (LATI-UEM) for realization of XRD analysis.

References

[1] Ahmed et al., "Eco-friendly biocatalysis: Innovative approaches for the sustainable removal of diverse dyes from aqueous solutions" Inorganic Chemistry Communications, 170, 113447, Nov. 2024, doi: 10.1016/J.INOCHE.2024.113447.

[2] Esparza et al., "Photodegradation of dye pollutants using new nanostructured titania supported on volcanic ashes" Applied Catalysis A: General, 388(1–2), 7–14, Jul. 2010, doi: 10.1016/J.APCATA.2010.07.058

[3] S. Mishra and B. Sundaram, "A review of the photocatalysis process used for wastewater treatment," Mater Today Proc, Jul. 2023, doi: 10.1016/J.MATPR.2023.07.147.

[4] F. C. Monteiro, I. D. L. Guimaraes, P. de Almeida Rodrigues, J. V. da Anunciação de Pinho, and C. A. Conte-Junior, "Degradation of PAHs using TiO2 as a semiconductor in the heterogeneous photocatalysis process: A systematic review," J Photochem Photobiol A Chem, vol. 437, p. 114497, Mar. 2023, doi: 10.1016/J.JPHOTOCHEM.2022.114497.

[5] M. Rehan and E. Elhaddad, "An efficient multi-functional ternary reusable nanocomposite based on chitosan@TiO2@Ag NP immobilized on cellulosic fiber as a support substrate for wastewater treatment," Environmental Pollution, vol. 340, p. 122850, Jan. 2024, doi: 10.1016/J.ENVPOL.2023.122850.

[6] Z. Yu, F. Li, and Q. Xiang, "Carbon dots-based nanocomposites for heterogeneous photocatalysis," J Mater Sci Technol, vol. 175, pp. 244–257, Mar. 2024, doi: 10.1016/J.JMST.2023.08.023.

[7] P. Karagoz, S. Khiawjan, M. P. C. Marques, S. Santzouk, T. D. H. Bugg, and G. J. Lye, "Pharmaceutical applications of lignin-derived chemicals and lignin-based materials: linking lignin source and processing with clinical indication," Biomass Conversion and Biorefinery 2023, vol. 1, pp. 1–22, Jan. 2023, doi: 10.1007/S13399-023-03745-5.

[8] E. Haque et al., "Recent advances in graphene quantum dots: Synthesis, properties, and applications," Small Methods, vol. 2, no. 10, pp. 1–14, Oct. 2018, doi: 10.1002/SMTD.201800050.

[9] T. Akhtar et al., "Fabrication of ruthenium doped Ag@TiO2 core-shell nanophotocatalyst for the efficient reduction of nitrophenols," Appl Surf Sci, vol. 630, p. 157491, Sep. 2023, doi: 10.1016/J.APSUSC.2023.157491.

[10] X. Wang et al., "Highly active Ag clusters stabilized on TiO2 nanocrystals for catalytic reduction of p-nitrophenol" Applied Surface Science, vol. 385, pp. 445–452, nov. 2016, doi: 10.1016/J.APSUSC.2016.05.147.

[11] J. C. M. Vicentini et al., "Photocatalytic water splitting with noble-metal free cocatalysts for a comprehensive study of two nonidentical photoreactors designs" Environmental Progress & Sustainable Energy, vol. 40, no. 3, 2021, doi: 10.1002/13557.

[12] L. Zhu, D. Li, H. Lu, S. Zhang, and H. Gao, "Lignin-based fluorescence-switchable graphene quantum dots for Fe3+ and ascorbic acid detection," Int J Biol Macromol, vol. 194, pp. 254–263, Jan. 2022, doi: 10.1016/J.IJBIOMAC.2021.11.199.

[13] E. Sehn, L. Hernandes, S. L. Franco, C. C. M. Gonçalves, and M. L. Baesso, "Dynamics of reepithelialisation and penetration rate of a bee propolis formulation during cutaneous wounds healing," Anal Chim Acta, vol. 635, no. 1, pp. 115–120, Mar. 2009, doi: 10.1016/J.ACA.2009.01.019.

[14] L. Bukman, C. F. de Freitas, W. Caetano, N. R. C. Fernandes, N. Hioka, and V. R. Batistela, "Kinetic spectrophotometric method for real-time monitoring of ultraviolet photoreactions: A mini-photoreactor," Spectrochim Acta A Mol Biomol Spectrosc, vol. 211, pp. 330–335, Mar. 2019, doi: 10.1016/J.SAA.2018.12.033.

[15] J. Yang, X. Yue, R. Zhang, and J. Ren, "Preparation of CQDs-TiO2 modified activated carbon with photocatalytic regeneration properties," Desalination Water Treat, vol. 222, pp. 271–281, May 2021, doi: 10.5004/DWT.2021.27086.

[16] J. Kong et al., "Carbon Quantum Dots: Properties, Preparation, and Applications," Molecules, vol. 29, no. 9, p. 2002, May 2024, doi: 10.3390/MOLECULES29092002.

[17] H. E. Hassan Ahmed and M. Soylak, "Exploring the potential of carbon quantum dots (CQDs) as an advanced nanomaterial for effective sensing and extraction of toxic pollutants," TrAC Trends in Analytical Chemistry, vol. 180, p. 117939, Nov. 2024, doi: 10.1016/J.TRAC.2024.117939.

[18] A. Bhosale, J. Kadam, T. Gade, K. Sonawane, and K. Garadkar, "Efficient photodegradation of methyl orange and bactericidal activity of Ag doped ZnO nanoparticles," Journal of the Indian Chemical Society, vol. 100, no. 2, p. 100920, Feb. 2023, doi: 10.1016/J.JICS.2023.100920.

[19] H. B. A. Sousa, C. S. M. Martins, and J. A. V Prior, "You Don't Learn That in School: An Updated Practical Guide to Carbon Quantum Dots," 2021, doi: 10.3390/nano11030611.

[20] P. Kumar, B. Sain, and S. L. Jain, "Photocatalytic reduction of carbon dioxide to methanol using a ruthenium trinuclear polyazine complex immobilized on graphene oxide under visible light irradiation," J Mater Chem A Mater, vol. 2, no. 29, pp. 11246–11253, Aug. 2014, doi: 10.1039/C4TA01494D.

[21] R. Bhargava and S. Khan, "Structural, optical and dielectric properties of graphene oxide," AIP Conf Proc, vol. 1953, May 2018, doi: 10.1063/1.5032346.

[22] A. Bansal et al., "Visible light-induced surface initiated atom transfer radical polymerization of methyl methacrylate on titania/reduced graphene oxide nanocomposite," RSC Adv, vol. 5, no. 27, pp. 21189–21196, 2015, doi: 10.1039/C4RA15615C.

[23] R. A. Spurr and H. Myers, "Quantitative Analysis of Anatase-Rutile Mixtures with an X-Ray Diffractometer," Anal Chem, vol. 29, no. 5, pp. 760–

762, 1957, doi: 10.1021/AC60125A006/ASSET/AC60125A006.FP.PNG_V03.
[24] Z. H. Dhoondia and H. Chakraborty, “Lactobacillus mediated synthesis of silver oxide nanoparticles,” Nanomaterials and Nanotechnology, vol. 2, no. 1, 2012, doi: 10.5772/55741.